DINAME 2017 - Proceedings of the XVII International Symposium on Dynamic Problems of Mechanics
A. T. Fleury, D. A. Rade, P. R. G. Kurka (Editors), ABCM, So Sebastio, SP, Brazil, March 5-10, 2017

# DYNAMIC BEHAVIOR AND OPTIMIZATION OF COMPOSITE TOW STEERED PLATES

**Thiago A. M. Guimarães[a], Daniel A. Pereira[b] and Domingos A. Rade[b]**

[a] School of Mechanical Engineering, Federal University of UberIndia, UberIndia, MG, Brazil
[b] Mechanical Engineering, Aeronautics Institute of Technology, São José dos Campos, SP, Brazil

*Abstract: In the last years, many techniques and procedures have been employed to optimize traditional constant stiffness composites laminates (CSCL). On the other hand, recent manufacturing methods enable to explore non conventional design approaches. The mechanism development of automatic fiber placement allows the design of variable stiffness composite laminates (VSCL), where the fibers are placed following a curvilinear trajectory. Differently from CSCL, the VSCL the stiffness is a function of the position on the laminate. VSCL can also be obtained considering variable fiber spacing, where the proportion of fiber and resign are not constant in the laminate. Some authors have explored the benefits of VSCL to improve buckling, to reduce stress concentrations around holes, to maximize the fundamental frequency in conical shells and even to optimize the aeroelastic behavior of composite wings. This work proposes a semi-analytical model to optimize a flat plate, controlling the angles in the interpolating positions in the laminate using Lagrange functions of different orders and for two different boundary conditions. A structural model based on Ritz method combined with the classical lamination theory to model the composite laminate is used. The plate is considered thin, modeled based on strain-displacement assumptions of Von-Karman, and the inertia terms are based on the hypotheses of Kirchhoff. The equations of motion are obtained from Lagranges equations. The modal properties (natural frequencies and mode shapes) are found by solving the associated eigenvalue problem. The proposed model is compared regarding fundamental frequencies and mode shapes are validated with a Nastran model. A convergence analysis is done to find the number of terms necessary in the Ritz series to converge the semi analytical model. The influence of the steering parameters on the fundamental frequency is examined. A differential evolution (DE) algorithm is used to optimize the fiber placement by controlling the interpolation points of Lagrange functions for different orders. The optimization aims to maximize the first natural frequency . In all the simulations, different configurations are tested: linear tow steered angle in one direction and steered plates interpolated by Lagrange functions of first order, second order and third order. Preliminary results show the maximization of the fundamental frequency by increasing the order of interpolation and also that as the polynomial order increases the fiber path become more complex and brings new challenges to manufacturing process. For all simulated conditions, one notices the benefits of VSCL in terms of the vibrational aspects, which leads to conclude that the design can be done properly for a specific purpose such as to avoid a specific range of excitation frequency, or to increase the aeroelastic stability margin.*

***Keywords: variable stiffness composite, optimization, plate vibration, eigenfrequencies***

## INTRODUCTION

Traditionally composite laminates are produced by stacking plies in a predefined constant direction choose by a certain design goal resulting in a constant stiffness composite laminate (CSCL). Notwithstanding, recently the variable stiffness laminates are being explored due the capability to stiffness control arranging fiber placement in a such away that improves design behavior for different purposes. Different procedures results in variable stiffness composite laminates (VSCL), by controlling fiber deposition by curved paths, or by adding micro carbon fiber (functional grade material fgm) or even though by using controlled spaces between during fiber deposition.

Nevertheless, as a result of the improvement of the automated fiber placement (AFP) technique tow steering has been developed to allow laminates to be constructed with variable angle tow (VAT) plies in which the fibers are placed following curvilinear paths, in such way that is possible to achieve additional structural design improvements (Parnas *et al.*, 2003) are gain attention of international literature. The use of VSCL can improve design characteristics in comparison with CSCL, without weight penalties Akhavan and Ribeiro (2016). Different works have been produced to demonstrate the benefits regarding structural behavior (Lopes *et al.* (2008), Gürdal *et al.* (2008), Kuo and Shiau (2009), Weaver *et al.* (2016)). Other studies are devoted to the vibrational and optimization of the dynamic characteristics (Akhavan and Ribeiro, 2011), Akbarzadeh *et al.* (2016), and aeroelastic (Stodieck *et al.* (2013), Stanford *et al.* (2014)) behavior of VAT flat plates.

CSCL optimization involves the task of finding for a combination of several straight-fibers with constant thicknesses aimed the best mechanical properties for different design purposes Ghiasi *et al.* (2010). In contradistinction the VSCL presents a higher optimization design cost due to the large number of design variables required to define the trajectory,

thicknesses and manufacturing constraints Wu *et al.* (2012).

This paper proposes a new evaluation approach to increase the fundamental frequency of tow steered composite laminates. The analysis results for several configurations are optimized and compared. A differential evolution (DE) algorithm is applied to optimize the tow steered composite plates providing promising results. The plate is modeled according to the Classical Lamination Theory (CLT), whereas Legendre polynomials are used as basis for the Ritz Method, being necessary smaller modifications to take into account different boundaries conditions. The fiber placement trajectory is specified by controlling points interpolated by Lagrange polynomials of different orders as proposed by Wu *et al.* (2012).

## FORMULATION

The plate is modeled based on strain-displacement assumptions of von-Karman, according to the Classical Lamination Plate Theory and each ply in plane strain, which means that all the out of plane strains are set to zero:

$$\gamma_{zx} = \gamma_{zy} = \epsilon_{zz} = 0 \tag{1}$$

The displacement field is represented as:

$$\begin{aligned} u(x,y,z,t) &= u_0(x,y,t) - z\frac{\partial w_0(x,y,t)}{\partial x} \\ v(x,y,z,t) &= v_0(x,y,t) - z\frac{\partial w_0(x,y,t)}{\partial y} \\ w(x,y,z,t) &= w_0(x,y,t) \end{aligned} \tag{2}$$

where $(u_0, v_0, w_0)$ are the displacements in the midplane.

Neglecting non-linear terms, the strain components are expressed by:

$$\epsilon = \left\{ \begin{array}{c} \epsilon_x \\ \epsilon_y \\ \gamma_{xy} \end{array} \right\} = \left\{ \begin{array}{c} \frac{\partial u_0(x,y,t)}{\partial x} - z\frac{\partial^2 w_0(x,y,t)}{\partial x^2} \\ \frac{\partial v_0(x,y,t)}{\partial y} - z\frac{\partial^2 w_0(x,y,t)}{\partial y^2} \\ \frac{\partial u_0(x,y,t)}{\partial x} + \frac{\partial v_0(x,y,t)}{\partial y} - 2z\frac{\partial^2 w_0(x,y,t)}{\partial y \partial x} \end{array} \right\} \tag{3}$$

where the linear membrane and out of plane terms are denoted as:

$$\epsilon^{\mathbf{L}} = \left\{ \begin{array}{c} \epsilon_x^L \\ \epsilon_y^L \\ \gamma_{xy}^L \end{array} \right\} = \left\{ \begin{array}{c} \frac{\partial u_0(x,y,t)}{\partial x} \\ \frac{\partial v_0(x,y,t)}{\partial y} \\ \frac{\partial u_0(x,y,t)}{\partial x} + \frac{\partial v_0(x,y,t)}{\partial y} \end{array} \right\} \tag{4}$$

$$\kappa = \left\{ \begin{array}{c} \kappa_x \\ \kappa_y \\ \kappa_{xy} \end{array} \right\} = - \left\{ \begin{array}{c} \frac{\partial^2 w_0(x,y,t)}{\partial x^2} \\ \frac{\partial^2 w_0(x,y,t)}{\partial y^2} \\ 2\frac{\partial^2 w_0(x,y,t)}{\partial x \partial y} \end{array} \right\} \tag{5}$$

Then, the forces (Q) and moments (B), with the assumptions of CLT, are:

$$\left\{ \begin{array}{c} \mathbf{Q} \\ \mathbf{B} \end{array} \right\} = \left[ \begin{array}{cc} \mathbf{A} & \mathbf{B} \\ \mathbf{B}^T & \mathbf{D} \end{array} \right] \left\{ \begin{array}{c} \epsilon^{\mathbf{L}} + \epsilon^{\mathbf{NL}} \\ \kappa \end{array} \right\} \tag{6}$$

in which, the membrane, membrane-bending, bending terms are given by the matrices ***A,B*** and ***D***. In the case of VAT plates, these matrices must be computed accounting for the fact that the ply angle varies over the plate according to Lagrange polynomials(Wu *et al.*, 2012):

$$\theta(x,y) = \Phi_i + \sum_{m=0}^{M-1}\sum_{n=0}^{N-1} T_{mn} \cdot \prod_{m \neq i} \frac{x - x_i}{x_m - x_i} \cdot \prod_{n \neq j} \frac{y - y_j}{y_n - y_j} \tag{7}$$

where $\Phi_i$ is the reference ply angle and $T_{mn}$ are the control angles in the reference points (M,N), as depicted in Fig. 1.

Considering symmetric laminates ***B=0***, the matrices ***A*** and ***D*** derived from a combination of in-plane and out-of-plane lamination parameters ($V_i$ and $W_i$).

$$(V_1, V_2, V_3, V_4)(x,y) = \frac{1}{h}\int_{-h/2}^{h/2} (cos(2\theta), sin(2\theta), cos(4\theta), sin(4\theta))dz \tag{8}$$

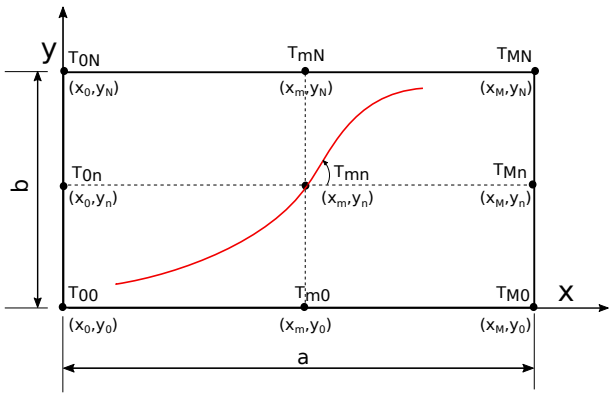


**Figure 1 – Non-Linear fiber orientation by Lagrange polynomials. (Adapted from (Wu *et al.*, 2012))**

$$(W_1, W_2, W_3, W_4)(x,y) = \frac{12}{h^3}\int_{-h/2}^{h/2} z^2(cos(2\theta), sin(2\theta), cos(4\theta), sin(4\theta))dz \tag{9}$$

and laminate invariants (Jones, 1998):

$$\begin{gathered}\Gamma_0 = \begin{bmatrix} I_1 & I_4 & 0 \\ I_4 & I_1 & 0 \\ 0 & 0 & I_5 \end{bmatrix}, \quad \Gamma_1 = \begin{bmatrix} I_2 & 0 & 0 \\ 0 & -I_2 & 0 \\ 0 & 0 & 0 \end{bmatrix}, \quad \Gamma_2 = \begin{bmatrix} 0 & 0 & I_2/2 \\ 0 & 0 & I_2/2 \\ I_2 & I_2 & 0 \end{bmatrix}, \\ \Gamma_3 = \begin{bmatrix} I_3 & -I_3 & 0 \\ -I_3 & I_3 & 0 \\ 0 & 0 & -I_3 \end{bmatrix}, \quad \Gamma_4 = \begin{bmatrix} 0 & 0 & I_3 \\ 0 & 0 & -I_3 \\ I_3 & -I_3 & 0 \end{bmatrix}\end{gathered} \tag{10}$$

are expressed by:

$$\begin{bmatrix} A_{11}(x,y) & A_{12}(x,y) & A_{16}(x,y) \\ A_{12}(x,y) & A_{22}(x,y) & A_{26}(x,y) \\ A_{16}(x,y) & A_{26}(x,y) & A_{66}(x,y) \end{bmatrix} = h(\Gamma_0 + \Gamma_1 V_1(x,y) + \Gamma_2 V_2(x,y) + \Gamma_3 V_3(x,y) + \Gamma_4 V_4(x,y)) \tag{11}$$

$$\begin{bmatrix} D_{11}(x,y) & D_{12}(x,y) & D_{16}(x,y) \\ D_{12}(x,y) & D_{22}(x,y) & D_{26}(x,y) \\ D_{16}(x,y) & D_{26}(x,y) & D_{66}(x,y) \end{bmatrix} = \frac{h^3}{12}(\Gamma_0 + \Gamma_1 W_1(x,y) + \Gamma_2 W_2(x,y) + \Gamma_3 W_3(x,y) + \Gamma_4 W_4(x,y)) \tag{12}$$

being $h$ the total thickness.

The strain energy of the composite plate may be expressed by:

$$U(x,y) = \frac{1}{2}\int_0^a \int_0^b \left\{\epsilon^L\right\}^T [\mathbf{A}] \left\{\epsilon^L\right\} dxdy + \frac{1}{2}\int_0^a \int_0^b \left\{\kappa^L\right\}^T [\mathbf{D}] \left\{\kappa^L\right\} dxdy \tag{13}$$

in the case of plate linear vibration the membrane terms has higher order frequency than the out of plane and can be simplified, resulting in:

$$U(x,y) = \frac{1}{2}\int_0^a \int_0^b \left\{\kappa^L\right\}^T [\mathbf{D}] \left\{\kappa^L\right\} dxdy \tag{14}$$

For the complete solution for different boundaries conditions the out of plane displacement can be written using Legendre polynomials, defined as:

$$\begin{gathered} L_0 = 1; \quad L_1 = x; \quad L_2 = \frac{1}{2}(3x^2 - 1)... \\ L_x = \sum_{j=0}^{J} (-1)^j \frac{(2i-2j)!}{2^i j!(i-j)!(i-2j)!} x^{i-2j} \\ J = \frac{i}{2} \quad (i = 0, 2, 4...), \quad \frac{i-1}{2} \quad (i = 1, 3, 5...) \end{gathered} \tag{15}$$

Choose following the work results of (**?**) work, in which was concluded that due the non-periodic nature of successive polynomials it is worth to capture localized effects. Nonetheless, it is necessary to modified the coordinates introducing the local normalized ones ($\zeta$ and $\eta$) defined as:

$$\zeta = x/a; \quad \eta = y/b; \tag{16}$$

the out of plane displacement for different boundaries conditions is defined:

$$w_0(\zeta,\eta,t) = (\zeta 2-\zeta)^c(\eta^2-\eta)^c \sum_{m_0}^{m_{max}} \sum_{n_0}^{n} q_{mn}(t) L_m(\zeta) L_n(\eta) \tag{17}$$

where c=0,1,2 defines boundaries conditions for all sides as free, simply supported and clamped respectively.

Thus the kinetic energy ($\Upsilon$), based on the hypotheses of Kirchhoff theory, which is adequate for thin plates one writes Love (1888):

$$\Upsilon = \frac{1}{2}\int\int\int \rho_0 \left[\dot{w}^2\right] dxdydz \tag{18}$$

being $\rho_0$ is the material density.

## Dynamic Model

The dynamic evaluation is done using Lagrange's equations (Lagrange, 2009) . Being $\vec{\mathbf{q}}$ the generalized coordinate that represents the displacements.

$$-\frac{\partial L}{\partial \mathbf{q}} + \frac{d}{dt}\left(\frac{\partial L}{\partial \dot{\mathbf{q}}}\right) = \mathbf{0} \tag{19}$$

where $L = \Upsilon - U$ is the Lagrangean function and $\mathbf{q}$ is the vector of generalized coordinates of out of plane displacement. Then the equation of motion for a condition free from external loads reads:

$$\mathbf{M}\ddot{\mathbf{q}} + \mathbf{K}\mathbf{q} = 0 \tag{20}$$

where $\mathbf{M}$ is the mass matrix, $\mathbf{K}$ is the structural stiffness.

Thus, the eigenvalues of the following eigenvalue problem represent the natural frequencies of the system:

$$\left(\mathbf{K} - \omega^2\mathbf{M}\right)\mathbf{q_w} = 0 \tag{21}$$

being the fundamental frequency the square root of the lowest eigenvalue found.

## MODEL DESCRIPTION AND VERIFICATION

Here next, it is presented the lamina properties and plate geometry. Then, it is presented the numerical model verification comparing the natural frequency and modes shapes from the Rayleigh Ritz (R.R.) model with the Nastran model.

It is evaluated a rectangular plate in tree different boundaries conditions, first the plate is assumed to be free in all four sides (FFFF), next all borders are simply supported (SSSS) and the last all borders are clamped (CCCC). The main dimensions are expressed in Fig. 2 and Table 1, where also is described the lamina properties.

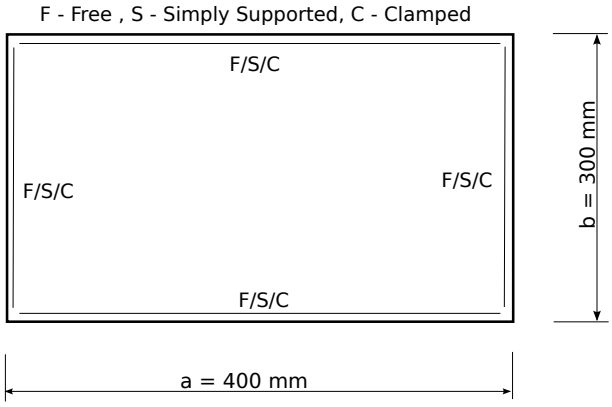


**Figure 2 – Plate Model Description**

The proposed model is compared regarding natural frequencies for the steered configuration (CA) and non steered configuration (CB) two different boundaries conditions. Also the mode shapes are compared for simple supported configuration (SSSS) evaluating the Modal Assurance criteria (MAC), which is portrayed in Fig. 3 where is possible to verify the agreement between modes obtained with Nastran and with the proposed model (RITZ).

**Table 1 – Material properties and plate dimensions**

| Property | Value | Property | Value |
|---|---|---|---|
| $E_1$ | 129500 MPa | Length, a | 400 mm |
| $E_2$ | 9370 MPa | Width,b | 300 mm |
| $G_{12}$ | 5240 MPa | Density,$\rho_0$ | 1500 kg/m$^3$ |
| $\mu_{12}$ | 0.38 | Ply thickness, t | 0.19 mm |

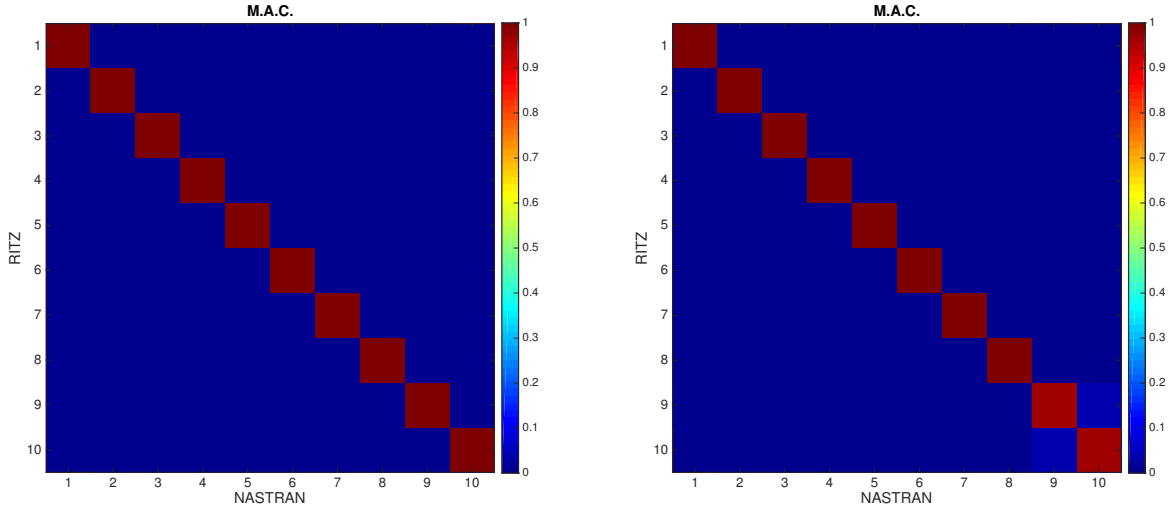


**Figure 3 – Mode Assurance Criteria for CA and CB**

In both configuration has the base lay-up defined by $[0^o/45^o/-45^o/90^o]_s$ . The difference in CB is related with the use of the second order Lagrange polynomials to perform a nonlinear interpolation in the laminate, following Eq. 7.

**Table 2 – Natural Frequencies comparison for different boundaries conditions of non-steered configuration CA**

| FFFF | | | SSSS | | | CCCC | | |
|---|---|---|---|---|---|---|---|---|
| **Ritz [Hz]** | **Nastran [Hz]** | **error %** | **Ritz [Hz]** | **Nastran [Hz]** | **error %** | **Ritz [Hz]** | **Nastran [Hz]** | **error %** |
| 41.65 | 41.31 | 0.83 | 64.36 | 63.88 | 0.75 | 117.89 | 116.82 | 0.92 |
| 63.77 | 62.96 | 1.28 | 153.82 | 152.47 | 0.88 | 230.42 | 227.77 | 1.17 |
| 81.23 | 80.54 | 0.85 | 168.59 | 166.97 | 0.97 | 250.19 | 247.07 | 1.26 |
| 103.54 | 101.76 | 1.75 | 253.56 | 248.68 | 1.96 | 349.30 | 340.78 | 2.50 |
| 118.75 | 116.76 | 1.70 | 313.31 | 309.94 | 1.09 | 407.58 | 412.92 | 1.29 |
| 192.67 | 188.13 | 2.41 | 336.30 | 333.02 | 0.98 | 418.56 | 444.20 | 5.77 |

**Table 3 – Natural Frequencies comparison for different boundaries conditions of steered configuration CB**

| FFFF | | | SSSS | | | CCCC | | |
|---|---|---|---|---|---|---|---|---|
| **Ritz [Hz]** | **Nastran [Hz]** | **error %** | **Ritz [Hz]** | **Nastran [Hz]** | **error %** | **Ritz [Hz]** | **Nastran [Hz]** | **error %** |
| 41.53 | 41.19 | 0.82 | 65.90 | 65.38 | 0.80 | 118.16 | 116.94 | 1.04 |
| 64.65 | 63.86 | 1.24 | 152.82 | 151.55 | 0.84 | 227.87 | 225.18 | 1.19 |
| 82.46 | 81.65 | 0.99 | 172.28 | 170.43 | 1.09 | 253.84 | 250.14 | 1.48 |
| 105.47 | 103.81 | 1.61 | 251.61 | 248.68 | 1.18 | 342.66 | 334.51 | 2.44 |
| 118.60 | 116.51 | 1.80 | 323.15 | 319.74 | 1.07 | 432.24 | 425.86 | 1.50 |
| 196.31 | 191.42 | 2.55 | 334.67 | 330.67 | 1.21 | 446.60 | 439.84 | 1.54 |

The proposed model converges with eight assumed modes in each direction and the frequency comparison is shown

in Table 2 and Table 3, in which has that FEM and RITZ models corroborates with an acceptable error. Also, the steered angle for the developed model and Nastran is depicted in Fig. 4.

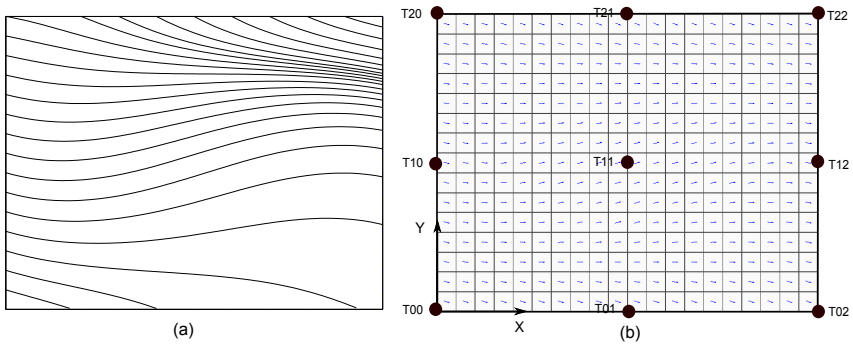


**Figure 4 – Steering Angle - a) Present Model; b) Nastran Model**

## OPTIMIZATION PROCEDURE

The Differential Evolution (DE) algorithm is used to determine the maximum fundamental frequency of tow steered plates in different boundaries conditions. Distinct optimizations are discussed, as presented in Fig. 5 and Table 4. All variables are considered continuous and lie inside the interval between $-90°$ and $90°$. Therefore, the optimization problem can be stated as:

Maximize: $\omega\_1$ $(First\ Fundamental\ Frequency)$
Design Variables: Table 4 in 2nd column
Subject to: T_mn $\in$ $[-90 \quad 90]$.

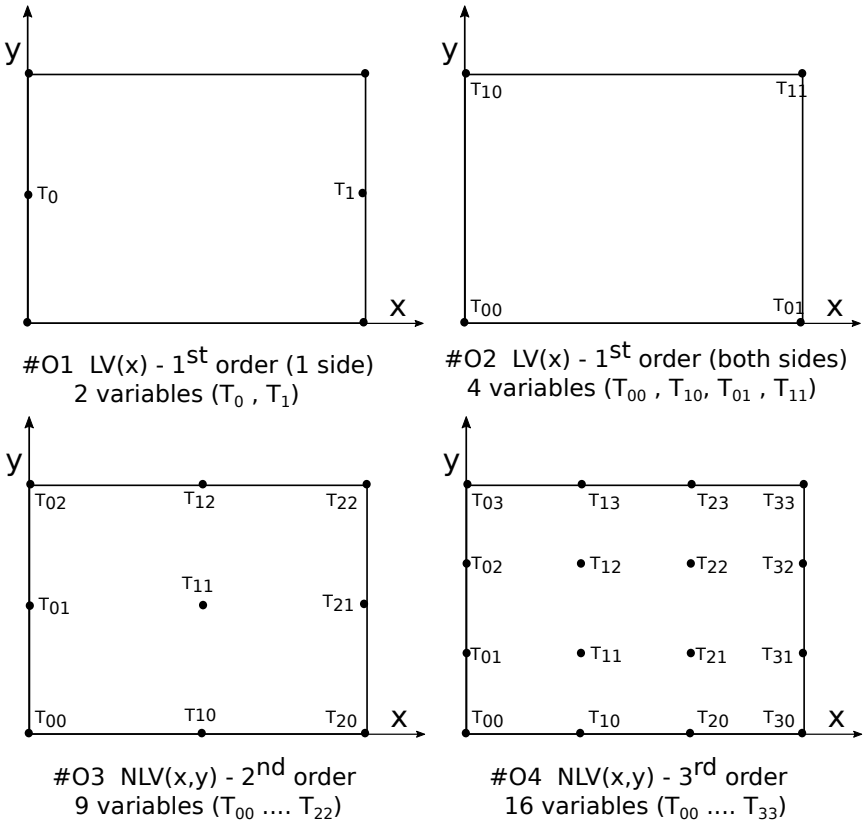


**Figure 5 – Design Space representation for different optimizations**

**Table 4 – Lay-up Options and Design Variables for Laminate [0 45 -45 90 ]$_s$**

| Configuration | Design Variables | Variables Type | Boundaries |
|---|---|---|---|
| $\#O1$ | $[T_0 \quad T_1]$ | Continuous | $[-90^0 \quad 90^0]_i$ |
| $\#O2$ | $\begin{bmatrix} T_{01} & T_{11} \\ T_{00} & T_{10} \end{bmatrix}$ | Continuous | $[-90^0 \quad 90^0]_i$ |
| $\#O3$ | $\begin{bmatrix} T_{02} & T_{12} & T_{22} \\ T_{01} & T_{11} & T_{21} \\ T_{00} & T_{10} & T_{20} \end{bmatrix}$ | Continuous | $[-90^0 \quad 90^0]_i$ |
| $\#O4$ | $\begin{bmatrix} T_{03} & T_{13} & T_{23} & T_{33} \\ T_{02} & T_{12} & T_{22} & T_{32} \\ T_{01} & T_{11} & T_{21} & T_{31} \\ T_{00} & T_{10} & T_{20} & T_{30} \end{bmatrix}$ | Continuous | $[-90^0 \quad 90^0]_i$ |

## ANALYSIS AND RESULTS

The results were organized in Table 5 separated by boundary condition. The baseline configuration was considered CA with fundamental frequency shown in Table 2. Though, the baseline fundamental frequency is 41.65Hz, 64.36Hz and 117.89Hz for free, simply supported and clamped configuration respectively.

**Table 5 – Natural Frequencies comparison for different boundaries conditions of steered configuration CB**

| | FFFF | | | SSSS | | | CCCC | | |
|---|---|---|---|---|---|---|---|---|---|
| | **Baseline [Hz]** | **Optimal [Hz]** | **Improve %** | **Baseline [Hz]** | **Optimal [Hz]** | **Improve %** | **Baseline [Hz]** | **Optimal [Hz]** | **Improve %** |
| #O1 | 41.65 | 45.15 | 8.40 | 64.36 | 78.53 | 22.02 | 117.89 | 153.64 | 30.32 |
| #O2 | | 47.24 | 13.42 | | 79.50 | 23.52 | | 154.03 | 30.66 |
| #O3 | | 47.49 | 14.02 | | 82.26 | 27.81 | | 160.06 | 35.77 |
| #O4 | | 48.60 | 16.69 | | 82.59 | 28.33 | | 160.20 | 35.89 |

As expected there was a direct relation between the path complexity (higher order polynomials) and the increasing of fundamental frequency. Actually, the smallest improvement was achieve in the SSSS condition (**16.7%**), increasing to (**28.3%**) for SSSS and the best results were found in the CCCC configuration (**36.0%**). The constraint effect is related with the potential energy evaluation (Eq. 13), which means that more constrained laminates has higher potential energy and higher frequencies. As a matter of fact, the effect of tow steered laminates allows the search in new design spaces, enhancing the evaluation of potential energy resulting in higher fundamental frequencies also, and the results tends to be better for constrained laminates.

In Fig. 6 is depicted the trajectory of each layer, being possible to compare for each condition the steered optimal with the baseline laminate.

Figures 7 to 9 presents the comparison between the baseline configuration and the optimal steered condition #O3 in the frequency domain for each boundary condition. Clearly it is shown the the increase of fundamental frequency in the VSCL.

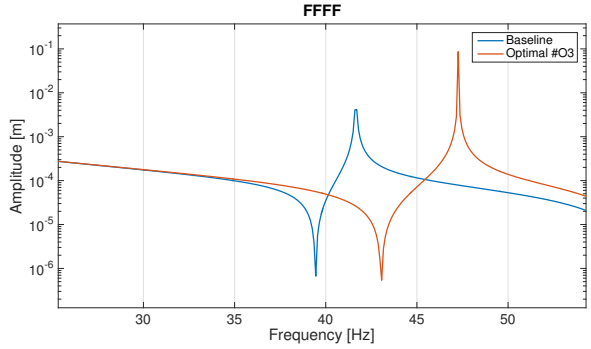


**Figure 7 – FFFF frequency response comparison between baseline configuration and optimal steered(#O3)**

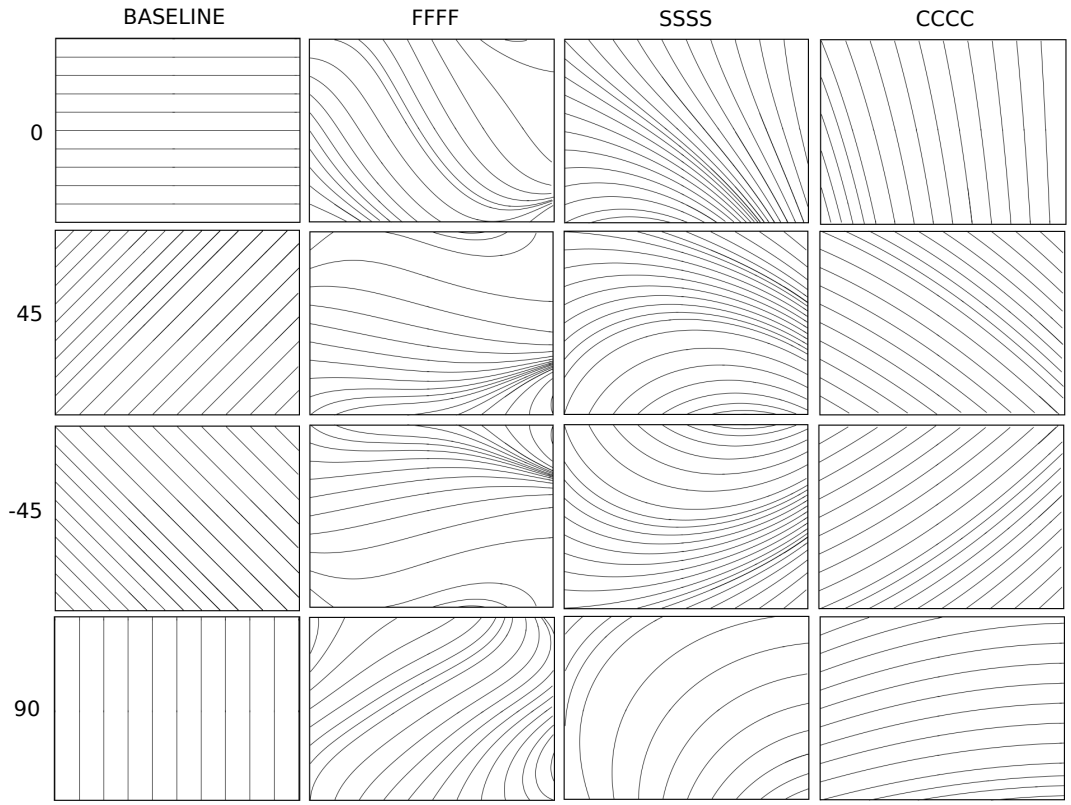


**Figure 6 – Optimal Trajectory Results Os resultados modifcaram um pouco (vou refazer esta figura)**

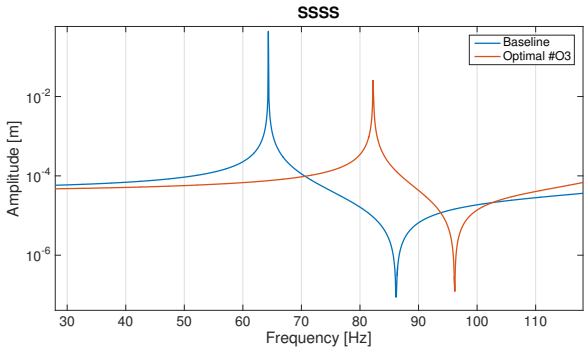


**Figure 8 – SSSS frequency response comparison between baseline configuration and optimal steered(#O3)**

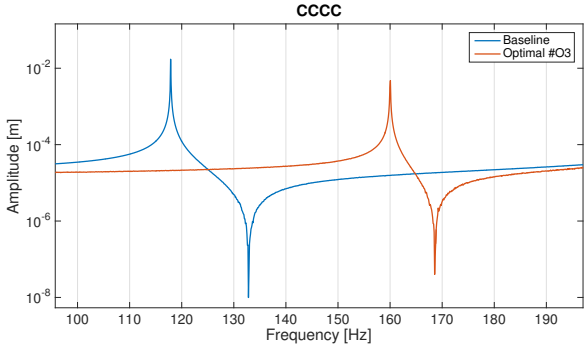


**Figure 9 – CCCC frequency response comparison between baseline configuration and optimal steered(#O3)**

## CONCLUSIONS

The deterministic optimization of symmetric tow steered composite plates was done for tree different boundaries condition (FFFF, SSSS, CCCC) aiming at increasing the fundamental frequency. The proposed model was validated for all boundaries conditions in terms of natural frequencies with a finite element model (FEM) done in Nastran®. In addition, the modal assurance criteria (MAC) evaluation was done to compare the modal characteristics of the developed model with the FEM showing a great correlation.

The use Lagrange interpolation polynomials to define tow steered angles was efficient to increase the first fundamental frequency, but as the complexity increased the computational effort to convergence also increased and the gain tends to be smaller for polynomials with order higher than two.

The condition FFFF presents smaller improvements than the condition SSSS and CCCC, which means that the constrained plays a important rule in the dynamic behavior of the tow steered plates. The geometry stiffness dependency is directly related with the potential energy evaluation, though it is possible state that constrained conditions is better to control tow steered angles improving the dynamic behavior by increasing the fundamental frequency.

The optimal steered paths became complex as the polynomial order increases, rising manufacturing issues. It is important to emphasize the importance of evaluating the influence of uncertainties affecting the VSCL for minimizing such influence on their structural and dynamic behaviors. This aspect is tightly related to the challenge of ensuring the necessary reliability under constraints and imperfections introduced by the manufacturing process.

## ACKNOWLEDGMENTS

The authors are thankful to Brazilian Research Agencies CNPQ, CAPES, FAPEMIG, FAPESP and the INCT-EIE for the continuous support to their research work.

## REFERENCES

Akbarzadeh, A.H., Arian Nik, M. and Pasini, D., 2016. "Vibration responses and suppression of variable stiffness laminates with optimally steered fibers and magnetostrictive layers". *Composites Part B: Engineering*, Vol. 91, pp. 315–326. doi:http://dx.doi.org/10.1016/j.compositesb.2016.02.003. URL http://www.sciencedirect.com/science/article/pii/S1359836816001037.

Akhavan, H. and Ribeiro, P., 2011. "Natural modes of vibration of variable stiffness composite laminates with curvilinear fibers". *Composite Structures*, Vol. 93, No. 11, pp. 3040 – 3047. ISSN 0263-8223. doi:http://dx.doi.org/10.1016/j.compstruct.2011.04.027. URL http://www.sciencedirect.com/science/article/pii/S0263822311001516.

Akhavan, H. and Ribeiro, P., 2016. "Geometrically non-linear periodic forced vibrations of imperfect laminates with curved fibres by the shooting method". *Composites Part B: Engineering*, pp. –. ISSN 1359-8368. doi:http://dx.doi.org/10.1016/j.compositesb.2016.10.059. URL http://www.sciencedirect.com/science/article/pii/S1359836816311726.

Ghiasi, H., Fayazbakhsh, K., Pasini, D. and Lessard, L., 2010. "Optimum stacking sequence design of composite materials part ii: Variable stiffness design". *Composite Structures*, Vol. 93, No. 1, pp. 1–13. doi:http://dx.doi.org/10.1016/j.compstruct.2010.06.001. URL http://www.sciencedirect.com/science/article/pii/S0263822310001947.

Gürdal, Z., Tatting, B. and Wu, C., 2008. "Variable stiffness composite panels: Effects of stiffness variation on the in-plane and buckling response". *Composites Part A: Applied Science and Manufacturing*, Vol. 39, No. 5, pp. 911 – 922. ISSN 1359-835X. doi:http://dx.doi.org/10.1016/j.compositesa.2007.11.015. URL http://www.sciencedirect.com/science/article/pii/S1359835X07002643.

Jones, R., 1998. *Mechanics of composite materials*. CRC.

Kuo, S.Y. and Shiau, L.C., 2009. "Buckling and vibration of composite laminated plates with variable fiber spacing". *Composite Structures*, Vol. 90, No. 2, pp. 196 – 200. ISSN 0263-8223. doi:http://dx.doi.org/10.1016/j.compstruct.2009.02.013. URL http://www.sciencedirect.com/science/article/pii/S0263822309000518.

Lagrange, J.L., 2009. *Mecanique Analytique:*, Vol. 1. Cambridge University Press, Cambridge. ISBN 9780511701788. doi:10.1017/CBO9780511701788.

Lopes, C., Gürdal, Z. and Camanho, P., 2008. "Variable-stiffness composite panels: Buckling and first-ply failure improvements over straight-fibre laminates". *Computers and Structures*, Vol. 86, No. 9, pp. 897 – 907. ISSN 0045-7949.

doi:http://dx.doi.org/10.1016/j.compstruc.2007.04.016. URL http://www.sciencedirect.com/science/article/pii/S0045794907001654. Composites.

Love, A.E.H., 1888. "The small free vibrations and deformation of a thin elastic shell". *Philosophical Transactions of the Royal Society of London A: Mathematical, Physical and Engineering Sciences*, Vol. 179, pp. 491–546. ISSN 0264-3820. doi:10.1098/rsta.1888.0016. URL http://rsta.royalsocietypublishing.org/content/179/491.

Parnas, L., Oral, S. and Ceyhan, A., 2003. "Optimum design of composite structures with curved fiber courses". *Composites Science and Technology*, Vol. 63, No. 7, pp. 1071–1082. ISSN 0266-3538. URL http://www.sciencedirect.com/science/article/pii/S0266353802003123.

Stanford, B.K., Jutte, C.V. and Chauncey Wu, K., 2014. "Aeroelastic benefits of tow steering for composite plates". *Composite Structures*, Vol. 118, pp. 416–422. ISSN 0263-8223. URL http://www.sciencedirect.com/science/article/pii/S0263822314003973.

Stodieck, O., Cooper, J.E., Weaver, P.M. and Kealy, P., 2013. "Improved aeroelastic tailoring using tow-steered composites". *Composite Structures*, Vol. 106, pp. 703–715. ISSN 0263-8223. URL http://www.sciencedirect.com/science/article/pii/S0263822313003462.

Weaver, P.M., Wu, Z.M. and Raju, G., 2016. "Optimisation of variable stiffness plates". In *Composite Materials and Structures in Aerospace Engineering*. Trans Tech Publications, Vol. 828 of *Applied Mechanics and Materials*, pp. 27–48. doi:10.4028/www.scientific.net/AMM.828.27.

Wu, Z., Weaver, P.M., Raju, G. and Chul Kim, B., 2012. "Buckling analysis and optimisation of variable angle tow composite plates". *Thin-Walled Structures*, Vol. 60, pp. 163–172. doi:http://dx.doi.org/10.1016/j.tws.2012.07.008. URL http://www.sciencedirect.com/science/article/pii/S0263823112001930.